Heliyon 10 (2024) e35930

Contents lists available at ScienceDirect

Heliyon

journal homepage: www.cell.com/heliyon

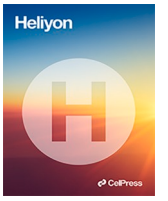

Research article

HAND2-AS1 plays a tumor-suppressive role in hepatoblastoma through the negative regulation of CDK1

Keke Chen [1], Yalan You [1], Wenfang Tang, Xin Tian, Chengguang Zhu, Zexi Yin, Minhui Zeng, Xiangling He [*]

Department of Pediatric Hematology and Oncology, School of Medicine, Children's Medical Center of Hunan Provincial People's Hospital of the First-Affiliated Hospital, Changsha, Hunan, 410005, China

ARTICLE INFO

Keywords:
HAND2-AS1
CDK1
Hepatoblastoma
Proliferation
Apoptosis
Cell cycle arrest

ABSTRACT

Objective: Hepatoblastoma (HB) is the most commonly seen pediatric liver malignancy. The preliminary experiment of our research group found that cyclin dependent kinase 1 (CDK1) was upregulated in HB. By in silico analysis, long noncoding RNA (lncRNA) HAND2 antisense RNA 1 (HAND2-AS1) was determined as the research object. Herein, HAND2-AS1 expression in HB and its effect and mechanism on HB were extensively investigated.

Methods: CDK1-related lncRNAs were searched using the microarray data from the Gene Expression Omnibus (GEO) database and Gene Expression Profiling Interactive Analysis (GEPIA) online database. qRT-PCR, Western blot, and immunohistochemistry were performed to determine the mRNA expression and protein levels of target genes. MTT, flow cytometry and DAPI staining assays were conducted to measure proliferation activity, cell cycle progression, and apoptosis of HB cells. The interaction between lncRNA and protein was determined by RNA pull-down and FISH assays. Luciferase assay was applied to identify whether HAND2-AS1 stimulates the transcription of CDK1. CDK1 mRNA stability was detected through actinomycin D assay. Aycloheximide assay was used to detect the CDK1 protein stability.

Results: HAND2-AS1 was downregulated in HB tissues and cells. HAND2-AS1 overexpression impeded HB cells proliferation activity and cycle progression while inducing cell apoptosis of HB cells, while knockdown of HAND2-AS1 emerged the opposite effect. HAND2-AS1 negatively correlated with CDK1. HAND2-AS1 downregulated CDK1 expression by affecting the transcriptional activity, mRNA and protein stability of CDK1. Furthermore, HAND2-AS1 impeded HB cell proliferation and cycle progression while inducing cell apoptosis by downregulating CDK1.

Conclusion: Our research highlights that HAND2-AS1 can exert a tumor-suppressive effect on HB through the negative regulation of CDK1, and the HAND2-AS1/CDK1 is expected to be a diagnostic molecular marker and therapeutic target for HB in clinical practice.

1. Introduction

Hepatoblastoma (HB) is the most common form of primary hepatic malignancy in the pediatric population, especially in infancy.

* Corresponding author.
E-mail address: hexiangling@hunnu.edu.cn (X. He).
[1] The authors contribute equally to this study.

https://doi.org/10.1016/j.heliyon.2024.e35930
Received 15 June 2023; Received in revised form 6 August 2024; Accepted 6 August 2024
Available online 8 August 2024

According to the statistics, HB patients under 5 years of age account for approximately 90 % of the total cases. The global incidence of HB has been increasing during the last few years. Nevertheless, the overall survival rate of HB is not optimistic, even with the continuous improvements in the technology of diagnosis and treatment. A complete surgical resection remains the standard intervention for HB patients. At the same time, adjuvant chemotherapy, neoadjuvant chemotherapy, or radiotherapy are alternatives to treatment for those patients with initially unresectable tumors [1]. However, the clinical efficacy of these alternatives is limited due to the unclear pathogenesis of HB. Therefore, exploring the pathogenesis of HB, developing molecular diagnostic indicators for HB, and seeking targeted drugs based on this have become the mainstream research trend of HB.

Cyclin-dependent kinases (CDKs) are a family of serine-threonine protein kinases playing a central role in the control of cell cycle progression [2]. Cyclin-dependent kinase 1 (CDK1), belonging to the CDK family, forms a complex with Cyclin A or Cyclin B under normal physiological conditions to regulate the G2/M transition of the cell cycle, and CDK1 loss could prevent cell division. Aberrant CDK1 activation has been proven to be a key factor for the initiation and progression of numerous malignancies [3]. For example, CDK1/2/5 kinase activity is critical for cytokine interferon-γ-mediated tumor immune evasion [4]. Qian et al. [5] have supported that KIAA1429 plays its oncogenic role in breast cancer through modulating CDK1 N6-methyladenosine-independently. As for HB, it has been reported that CDK1 is expected to be a potential biomarker for HB [6,7]. Notably, CDK1 inhibitor treatment of MYC-dependent mouse lymphoma and HB tumors retards tumor growth and prolongs survival [8]. In addition, a previous investigation by our group (data unpublished) showed that the expression level of CDK1 was remarkably increased in HB tissue samples than in adjacent normal tissue samples. Thus, the present study will continue to explore the role and mechanism of CDK1 in HB.

Non-coding RNAs (ncRNAs), once considered the junk of gene transcriptomes, have aroused wide concern because of their key roles in regulating cell physiological activities [9,10]. Long non-coding RNAs (lncRNAs) can modulate gene transcription in the nucleus and affect protein translation in the cytoplasm [11]. Outside the cells, lncRNAs can also enter the interstitial fluid through the action of exosomes, which could be used as a tumor marker to facilitate the early diagnosis of tumors [12,13]. Among which, lncRNA heart and neural crest derivatives expressed 2-antisense RNA 1 (HAND2-AS1) was found to be abnormally expressed in various tumors and be involved in the regulation of disease development. For instance, Gao et al. [14] have found that HAND2-AS1 might play suppressive roles in the occurrence and progression of cervical tumor cells via modulating the miR-21–5p/TIMP3/VEGFA axis. Another study has revealed that HAND2-AS1 is upregulated in hepatocellular carcinoma (HCC), promoting liver cancer stem cell self-renewal and ultimately driving HCC initiation [15]. However, the expression and function of HAND2-AS1 in HB are still in their infancy.

In this study, ncRNAs related to CDK1 expression were screened through the Gene Expression Omnibus (GEO) microarray data GSE131329, Gene Expression Profiling Interactive Analysis (GEPIA) database was employed to verify the correlations of these ncRNAs with CDK1 expression, and finally, HAND2-AS1 was determined as the research object through a series of experimental verification. Collectively, this study provided evidence that HAND2-AS1 expression was decreased in HB, and HAND2-AS1 overexpression could impede cell proliferation and cycle while inducing cell apoptosis via negatively regulating CDK1. This research highlights that the HAND2-AS1/CDK1 might be an underlying diagnostic marker and therapeutic target for HB.

2. Materials and methods

2.1. Clinical sampling

A total of 20 hepatoblastoma and matched adjacent non-tumor tissue samples were obtained from the patients who undergo routine surgery in Hunan Provincial People's Hospital. All tissues were fixed in formalin or snap-frozen in liquid nitrogen and kept at −80 °C before use. This study was performed under the review and approval of the Ethics Committee of Hunan Provincial People's Hospital (approval no. 2021-77) and written informed consent was obtained from all patients enrolled. The clinical information was listed in Table S1.

2.2. Bioinformatic analysis

The HB microarray data GSE131329 and GSE75271 [16] were downloaded from the GEO database (https://www.ncbi.nlm.nih.gov/gds/). The interactions between ncRNAs and CDK1 were predicted by the online RNACT database (https://rnact.crg.eu/) [17]. The GEPIA database (http://gepia.cancer-pku.cn/index.html) [18] was employed to further validate the differential expression and survival analysis of HAND2 in The Cancer Genome Atlas (TCGA) database.

2.3. Cell culture

Human HB cell lines [HepG2 (SCSP-510), HuH-6 (SCSP-5205)] and non-malignant hepatocyte cell line THLE-2 (SCSP-5068) were procured from the Shanghai Cell Bank of the Chinese Academy of Sciences (Shanghai, China). HepG2 cells were cultivated in minimum essential medium (MEM) medium (11095080, Gibco, Grand Island, NY, USA) supplemented with 1 % non-essential amino acids solution (11140050, Gibco). HuH-6 cells were cultured in DMEM medium (11995065, Gibco). THLE-2 cells were cultured in Bronchial Epithelial Cell Growth Medium (CC-3170, Lonza Group Ltd., Basel, Switzerland) supplemented with 10 % FBS, 1 % penicillin-streptomycin, 5 ng/mL EGF and 70 ng/mL Phosphoethanolamine. All cells were cultured at 37 °C in a humidified atmosphere containing 5 % CO_2. The media was renewed every 2–3 days and passaged at 1:2.

2.4. Quantitative reverse transcription-polymerase chain reaction (qRT-PCR)

Hepatoblastoma and matched adjacent non-tumor tissues (about 100 mg) and confluent cells after transfection (about 3×10^6 per well of six-well plate) were harvested for RNA isolation. Tissues were ground in liquid nitrogen. The cells were collected with cell scraper and washed once with ice-cold PBS. Then, 1 mL of TRIzol reagent (15596026, Invitrogen, Carlsbad, CA, USA) was added into the tissue or cell samples for RNA isolation according to the manufacturer's protocol. The concentration of RNA was measured by a NanoDrop microvolume spectrophotometer (701–058112, Thermo Fisher Scientific, Waltham, MA, USA). A reverse transcription kit (RR037B, TaKaRa, Tokyo, Japan) was used to reversely transcribe RNA (about 1 μg) as per the kit's protocols. A fluorescence quantitative PCR kit (SYBR Green Mix, Roche Diagnostics, Indianapolis, IN, USA) was employed to test the gene expression. The protocols of the fluorescence quantitative PCR instrument (LightCycler 480, Roche Diagnostics) were followed to set the reaction conditions. The PCR temperature cycling conditions were as follows: initial denaturation at 95 °C for 3 min; 35 cycles of denaturation at 95 °C for 15 s, annealing at 60 °C for 15 s, and elongation at 72 °C for 30 s. The final cycle was followed by extension at 72 °C for 5 min. Quantitative PCR was conducted in 3 replicates per reaction. Glyceraldehyde phosphate dehydrogenase (GAPDH) was considered as an internal control. $2^{-\Delta\Delta Ct}$ method was applied to analyze data: $\Delta\Delta Ct$ = experimental group ($Ct_{\text{target gene}}$ - $Ct_{\text{internal reference}}$) - control group ($Ct_{\text{target gene}}$ - $Ct_{\text{internal reference}}$). The primer sequences of each gene for PCR amplification and its internal control are detailed in Table 1.

2.5. Cell transfection

Two HAND2-AS1 shRNA vehicles (sh-HAND2-AS1#1 and sh-HAND2-AS1#2) and its shRNA negative control (sh-NC), pcDNA3.1-HAND2-AS1, pcDNA3.1-CDK1 and its corresponding negative control (vector) were purchased from Ori-Bio tech (Changsha, China). The HuH-6 cells were plated in 6-well plates at a density of 1×10^6 per well and cultured in incubator for 24h at 37 °C in 5 % CO_2 until the cell confluence arrived 70%–80 %. Then, the cells were transfected with vectors (final concentration 2 μg/mL) for 48 h following the requirements of Lipofectamine 3000 reagent (L3000150, Invitrogen). The transfected cells were collected for functional experiments and extraction of cellular RNA for qRT-PCR assay and total protein for Western blot analysis. Cell groups were named with their transfected shRNA or plasmid. The sequences of overexpressing vector of HAND2-AS1 and CDK1 and shRNA vector of HAND2-AS1 are listed in Table 1.

Table 1
The primer sequences for the study.

	Name		Sequences (5′-3′)
qRT-PCR primer sequences	HAND2-AS1	Forward	TAGTCCAGTGTGGTGGAATT CGATTGGCTACCTCCTCATAACCA
		Reverse	AACGGGCCCTCTAGACTCGAGTTAGA TTCTGTAATTTTATTACTGACATCATC
	CDK1	Forward	GGATGTGCTTATGCAGGATTCC
		Reverse	CATGTACTGACCAGGAGGGATAG
	GAPDH	Forward	GGAGCGAGATCCCTCCAAAAT
		Reverse	GGCTGTTGTCATACTTCTCATGG
Vector primer sequences	pcDNA3.1-HAND2-AS1	Forward	CTAGCGTTTAAACTTAAGCTTAA ATAAATACTAATGCGAGGATAATGC
		Reverse	TGCTGGATATCTGCAGAATTCTTTT TTTTTTTTTTTTTAGATTCTGTAATTT
	pcDNA3.1-CDK1	Forward	CTAGCGTTTAAACTTAAGCTTATGGA AGATTATACCAAAATAGAGAAAATT
		Reverse	TGCTGGATATCTGCAGAATTCCTACAT CTTCTTAATCTGATTGTCCAAA
	sh-NC	Forward	GATCCGCAGATGAAGGCACGGTCACGCTC GAGGCAGATGAAGGCACGGTCACGTTTTTG
		Reverse	AATTCAAAAAGCAGATGAAGGCACGGTCAC GCTCGAGGCAGATGAAGGCACGGTCACGG
	sh-HAND2-AS1#1	Forward	GATCCGTTTAACTAGCCTGTTTGAAGCTCGA GCTTCAAACAGGCTAGTTAAACTTTTTG
		Reverse	AATTCAAAAAGTTTAACTAGCCTGTTTGAAG CTCGAGCTTCAAACAGGCTAGTTAAACG
	sh-HAND2-AS1#1	Forward	GATCCGGATTAAGCTGGAATAATAAACTC GAGTTTATTATTCCAGCTTAATCCTTTTTG
		Reverse	AATTCAAAAAGGATTAAGCTGGAATAATA AACTCGAGTTTATTATTCCAGCTTAATCCG
	CDK1 promoter vector	Forward	AATTCTAGGCGATCGCTCGAGTTA TACAATTTCCTCTGTATGGAAGGC
		Reverse	ATTTTATTGCGGCCAGCGGCCGC AGAGAAAAAGCAGGAGGGCG

2.6. 3-(4,5-Dimethyl-2-thiazolyl)-2,5-diphenyl-2-H-tetrazolium bromide (MTT) assay

The well-grown cells were made into cell suspension with a cell concentration of 10^5 cells/mL. The 96-well cell culture plate, with an addition of 100 μL of the cell suspension to each well (about 10^4 cells/well), was placed in the incubator for culture. Forty-eight hours later, the 96-well cell plate was taken out and an MTT solution (M1025, Solarbio, Beijing, China) of 10 μL was added to each well. The culture medium was discarded 4 h later, and dimethyl sulfoxide solution (DMSO, 100 μL) was subsequently supplemented. Lastly, a microplate reader was used to analyze the optical density at 570 nm.

2.7. Flow cytometry assay for cell apoptosis

The HuH-6 cells were seeded onto 6-well plates, followed by cell transfection treatment according to the above scheme. Next, cells were collected, rinsed two times in cold phosphate-buffered saline (PBS), and annexin V-fluorescein isothiocyanate (FITC)/propidium iodide (PI) apoptosis kit (AT101-100, MultiSciences [Lianke] Biotech, Co., Ltd., Hangzhou, China) as per the manufacturer's protocol. Breifly, about 1×10^5 cells were suspended in 500 μL binding buffer and flow cytometry (C6, BD Biosciences, San Jose, CA, USA) were carried out to evaluate cell apoptosis. The analysis gates were drawn by using the negative control (unstained blank cells). The FlowJo software (BD) was used for data analysis. The apoptosis rate was calculated as the percentage of (Q2 + Q4). Q2: Annexin V-FITC positive/PI positive; Q4: Annexin V-FITC positive/PI negative.

2.8. DAPI staining for cell apoptosis

DAPI (4′6-Diamidino-2-phenylindole) staining was applied to apoptosis evaluation at a morphological level based on previous researches [19,20]. In short, 1.5×10^4 of HuH-6 cells were seeded into 96-well plates. After passing the incubation time for 24 h at 37 °C, the cells washed by PBS and then fixed with 4 % paraformaldehyde for 20 min. After that, the cells were washed with PBS, 0.3 % Triton X-100 was used to permeabilization for 10 min, and the cells were incubated for 10 min by 10 μg/mL DAPI. Eventually, the cells were washed with PBS and evaluated by a fluorescent microscope (Olympus, Tokyo, Japan).

2.9. Cell cycle analysis

The cell cycle staining kit (CCS012, MultiSciences [Lianke] Biotech) was employed to analyze the cell cycle as per the manufacturer's instructions. In short, HuH-6 cells were subjected to cell transfection treatment, collected, and rinsed two times in cold PBS. Next, 70 % ethanol was applied to fix cells overnight. After that, cells were subjected to 30-min staining with 50 μL/mL propidium iodide (PI)-contained binding buffer away from light, and then a flow cytometer (C6, BD Biosciences) was immediately used to analyze cell cycle within 30 min. The FlowJo software (BD Biosciences) was used for data analysis.

2.10. Immunohistochemistry (IHC)

The hepatoblastoma and matched adjacent non-tumor tissues were embedded in paraffin and each paraffin was cut into 4-μm-thick sections. Next, sections were routinely deparaffinized, rehydrated in alcohol with gradient concentrations, and subjected to antigen retrieval by Tris-EDTA antigen retrieval solution (P0084, Beyotime, Shanghai, China), blocking endogenous peroxidase by 3 % H_2O_2, and immunol staining blocking solution (P0102, Beyotime) for non-specific binding blockage, followed by antibody incubation with the primary antibody against CDK1 (ab18, 1:50, Abcam, Cambridge, UK). After overnight incubation at 4 °C in wet box, the sections were rinsed with PBS for 3 times and then subsequent steps were completed using an universal two-step detection kit (PV-9000, ZSGB-BIO, Beijing, China) and 3,3′-diaminobenzidine (DAB) chromogenic solution. Briefly, sections were incubated with reaction enhancer reagent at 37 °C for 20 min and further incubated with enhanced enzyme-labeled goat anti-mouse/rabbit IgG polymer at 37 °C for 20 min. Finally, the sections were stained with fresh prepared DAB solution for 5–8 min at room temperature. The nuclei were re-stained by hematoxylin. The sections were observed by an optical microscope (BX53, Olympus). The Immunohistochemical evaluation criteria are listed in Table 2.

2.11. RNA pull-down assay

RNA pull-down experiments were implemented using the HAND2-AS1 probe in HuH-6 cells based on previous research [21]. Briefly, 3 μg of biotin-labeled RNA was added with Structure Buffer to form secondary structures. After that, the pretreated magnetic

Table 2
Immunohistochemical evaluation criteria.

Positive cells (%)	Scores	Staining intensity	Scores
0–10	0	None	0
10–25	1	Weak (light yellow)	1
25–50	2	Moderate (brownish yellow)	2
50–100	3	Strong (dark brown)	3

beads were added to the biotin-labeled RNA, followed by a 1-h incubation at room temperature. The magnetic bead-RNA mixture was supplemented with cell lysate and an appropriate amount of RNase inhibitor, followed by another 1-h incubation at room temperature. Subsequently, the incubated magnetic bead-RNA-protein mixture, with the removal of the supernatant, was rinsed with RIP Buffer 5 times. The magnetic beads were eluted for 15 min on a mixer at room temperature and then put in a magnetic separator. The liquid transferred to a new EP tube was the eluate product. Lastly, the eluate product was added with 2 × SDS loading buffer, denatured at 95 °C for 10 min, and then subjected to immunoblotting detection.

2.12. Luciferase assay

The fragement of CDK1 promoter was synthesized and cloned into the downstream of Renilla of psiCHECK-2 luciferase reporter plasmid (C8021, Promega, Madison, USA) according to manufacturer's guidance and previous research [22]. Then, HuH-6 cells were cultured in a 24-well plate and then transfected with pcDNA3.1-HAND2-AS1 and the luciferase reporter plasmid (C8021, Promega). The luciferase activity was evaluated using the Dual-Luciferase Assay Kit (E1910, Promega). After 48 h post-transfection, the cell medium was removed and HuH-6 cells were washed twice with PBS, followed by the treatment with 100 μL of passive lysis buffer. The culture plates were gently shaken for 15 min at room temperature and cell lysates were collected. Cell lysate (20 μL) was transferred into the luminometer tube containing Luciferase Assay Reagent II (100 μL) and was mixed by pipetting two or three times. The Firefly luciferase activity was was detected with a microplate reader (GM3500; Promega). Stop & Glo® Reagent (100 μL) was added to the tube and vortexed briefly to mix; and the Renilla luciferase activity was measured by a microplate reader (GM3500; Promega). The firefly luciferase activity was normalized to Renilla luciferase activity.

2.13. mRNA stability analysis

At 48 h after transfection with pcDNA3.1-HAND2-AS1 and its vector control into HuH-6 cells, actinomycin D (ActD, SBR00013, 5 μg/mL, Sigma-Aldrich, St. Louis, USA) were added into the culture medium and further culture for 0, 2, 4, or 8 h [23], respectively. Then, total RNA was extracted from HuH-6 cells at each time point, and CDK1 mRNA level was measured through qRT-PCR assay.

2.14. Protein stability analysis

Protein synthesis was inhibited by treatment with cycloheximide (CHX, Sigma-Aldrich) at a concentration (25 μg/mL) for 0-, 2-, 4-, and 8-h culture. Then, total protein was isolated. The changes in CDK1 protein half-life were detected by performing Western blot analysis [24].

2.15. Western blot analysis

HuH-6 cells were lysed using Radioimmunoprecipitation assay lysis buffer (P0013B, Beyotime) was employed to lyse cells for protein extraction. After the measurement of the protein concentration with A bicinchoninic acid assay (BCA) protein assay kit (P0010, Beyotime) was applied to measure the protein level, and the loading buffer (P0015L, Beyotime) was added to the protein samples for later use. Afterward, the 80 μg protein samples separated by sodium dodecyl sulfate-polyacrylamide gel electrophoresis were transferred to the Polyvinylidene Fluoride (PVDF) membranes. Then, the blocking solution (P0023B, Beyotime) was applied to block PVDF membranes at ambient temperature for 60 min, followed by incubation at 4 °C overnight with the primary antibody against GAPDH (5174S, 1: 1000, Cell Signaling, Boston, USA), CDK1 (ab18, 1: 500, Abcam), Cyclin D1 (# 55506, 1: 1000, Cell Signaling), and Cyclin B1 (# 4138, 1: 1000, Cell Signaling). Next, the PVDF membrane was washed thrice with Tris-buffered saline with Tween-20 (TBST) for 10 min each time. The membrane was incubated with a secondary antibody (horseradish peroxidase-conjugated goat anti-rabbit or mouse IgG, 1:5000, CW0103 and CW0102 Beijing ComWin Biotech Co., Ltd.) for 1 h, followed by washing thrice with TBST for 10 min each time. Lastly, the membrane was developed by the enhanced chemiluminescent reagent (P0018S, Beyotime), and the chemiluminescence imaging system (Tanon-5200, Tanon, Shanghai, China) was used for detection. The high-resolution images of all blots were showed in the Supplementary Material_1.

2.16. Immunofluorescence staining combined RNA fluorescence in situ hybridization (FISH)

HuH-6 cells (2×10^5) seeded onto 6-well plates with coverglass in the well. Twenty-four hours later, the coverglass with cells grown on it were fixed in 4 % formaldehyde for 30 min, and then rinsed with PBS. After permeabilization by 0.2 % Triton-X100 (93443, Sigma-Aldrich) in PBS for 20 min and three washes with PBS, cells were incubated with 5 % goat serum to block non-specific sites. Then, cells were incubated with anti-CDK1 at 4 °C overnight and HRP-labeled secondary antibody at ambient for 50 min. Cells were further incubated with TSA-520 at 37 °C for 20 min. Finally, cells digested with proteinase K were prehybridized with a hybridization buffer, followed by incubation with Cy5-labeled HAND2-AS1 probes in hybridization solution. Cell nuclei were stained with DAPI for 5 min at ambient temperature. Finally, antifade mounting medium (P0126, Beyotime) was added into cells. A fluorescence microscopy (BX53, Olympus) was utilized to obtain fluorescence images. Blue fluorescence indicated the cell nucleus stained with DAPI (excitation 360 nm/emission 460 nm), red fluorescence indicated Cy5-labeled HAND2-AS1 (excitation 633 nm/emission 670 nm), green fluorescence indicated CDK1 expression (excitation 490 nm/emission 520 nm)

2.17. Statistical analysis

The cell experiments were performed for three biological replicates (each biological replicate included three technical replicates). All the experimental data were expressed as mean ± standard deviation (SD). A *t*-test or one-way analysis of variance (ANOVA) was

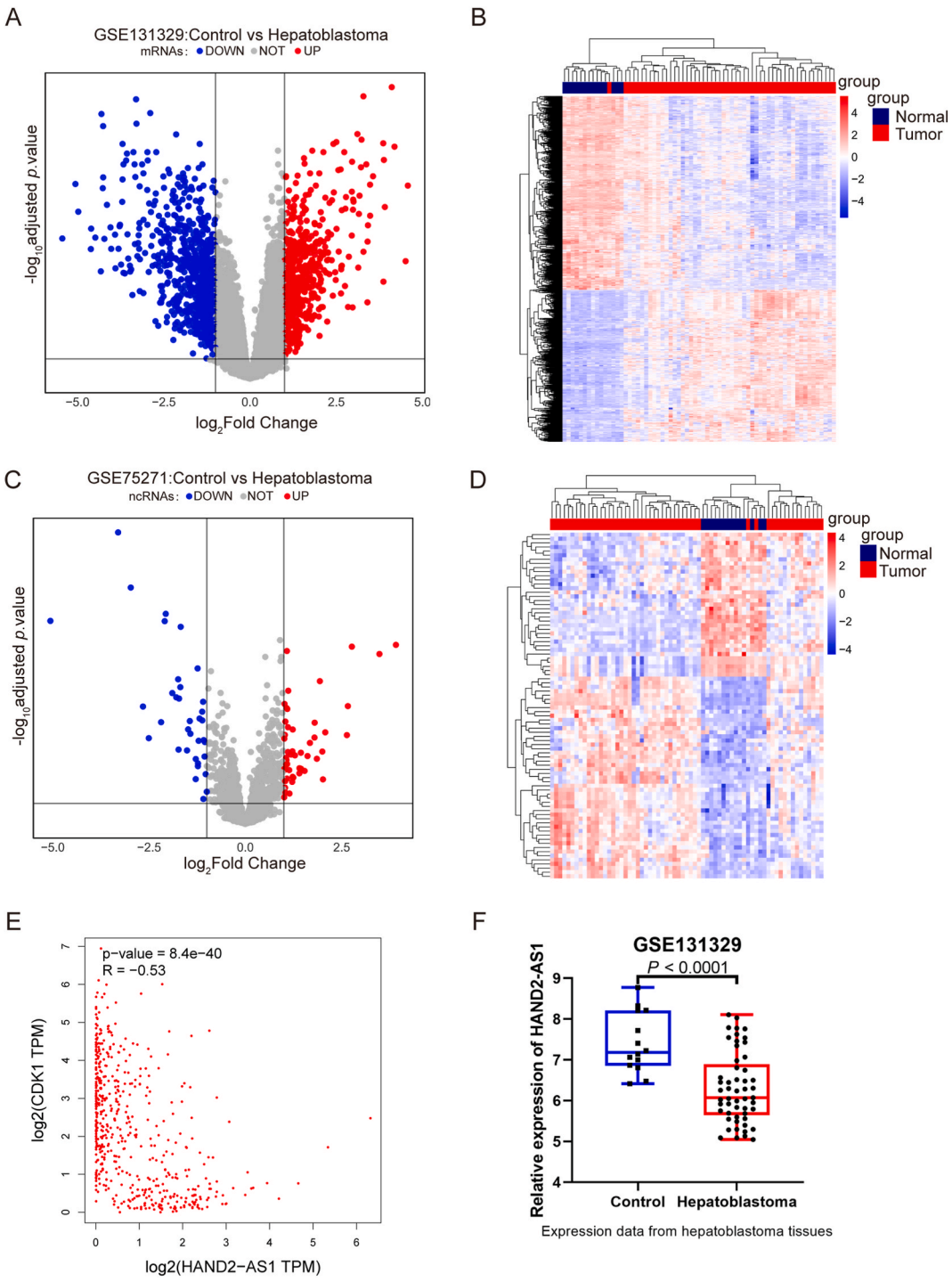

Fig. 1. Screening of CDK1-related genes. A-B. Differentially expressed genes in microarray data GSE131329 were shown in volcano plots and heatmaps, respectively. C-D. Differentially expressed ncRNAs in microarray data GSE131329 were shown in volcano plots and heatmaps, respectively. E. GEPIA database exhibited that HAND2-AS1 expression in liver tissues (normal + tumor) was negatively correlated with CDK1 expression. F. GSE131329 microarray data showed reduced HAND2-AS1 expression in HB.

performed using Graphpad Prism 8.0 software. Multiple comparisons of the means of each group were conducted using the Turkey method. The significance level was set at $P < 0.05$. The experimental raw data of the study were listed in the Supplementary Material_2.

3. Results

3.1. Screening of CDK1-related genes

Microarray data GSE131329, including 14 non-HB liver tissues and 53 HB tissues, yields 23,307 genes using 33,297 probes. Using the R language limma package (version.3.44.3) and the threshold of log |FC| > 1 and adjusted $P < 0.05$, 777 downregulated and 610 upregulated genes were obtained after analysis (Fig. 1A–B). The microarray data contained 4187 detected ncRNAs; 35 ncRNAs were significantly downregulated, and 49 ncRNAs were upregulated with the threshold of log |FC| > 1 and adjusted $P < 0.05$ (Fig. 1C–D). The previous investigation of our group suggested that CDK1 was upregulated in HB (unpublished). Given this, the interaction of these 84 differentially expressed ncRNAs with CDK1 was predicted using the online RNACT database (https://rnact.crg.eu/) with the Prediction Score >15. Finally, 6 ncRNAs in Table 3 were found to be able to bind to CDK1 and the potential binding sites of these 6 lncRNAs within CDK1 were provided in Table S2 by RNA-Protein Interaction Prediction (RPISeq, http://pridb.gdcb.iastate.edu/RPISeq/).

Next, the correlation between CDK1 expression and expression of these 6 ncRNAs in cancer and non-cancer tissues was explored with the online GEPIA database (http://gepia.cancer-pku.cn/). HAND2-AS1 had the strongest negative correlation with CDK1 (Fig. 1E). Therefore, HAND2-AS1 was selected as the research object for further exploration. Similarly, the results of the microarray data GSE131329 were consistent with those of the GEPIA database, which highlighted that the expression level of HAND2-AS1 expression was down-regulated in HB (Fig. 1F). In summary, HAND2-AS1 is down-regulated in HB and negatively correlates with CDK1 expression.

3.2. The expression level of HAND2-AS1 in HB tissues and cell lines

Subsequently, qRT-PCR was performed to examine the expression level of HAND2-AS1 within our collected HB tissues and their corresponding adjacent normal tissues. Fig. 2A demonstrated that HAND2-AS1 expression was dramatically decreased within HB tissue samples than paired adjacent normal tissue samples ($n = 20$; $P < 0.001$; Table S3). Meanwhile, HAND2-AS1 expression in HB cell lines (HepG2 and HuH-6) and non-malignant hepatocyte cell line THLE-2 was tested by qRT-PCR, which demonstrated a low HAND2-AS1 expression in HB cells when compared to THLE-2 cells (all $P < 0.001$, Fig. 2B; Table S4). Therefore, HAND2-AS1 is downregulated in HB.

3.3. Effects of HAND2-AS1 on proliferation, cycle arrest, and apoptosis of HB cells

Subsequently, shRNA and overexpression plasmids were constructed to knock down and overexpress HAND2-AS1, respectively, with the transfection efficiency verified by qRT-PCR. Fig. 3A–B and Table S5 exhibited a good transfection efficiency of sh-HAND2-AS1-1 ($P < 0.001$), sh-HAND2-AS1-2 ($P < 0.001$), and the overexpression plasmid HAND2-AS1-vector ($P < 0.01$). The roles of HAND2-AS1 in the biological functions of HB cells were investigated. The transfection of sh-HAND2-AS1-1 and sh-HAND2-AS1-2 in HB cells enhanced proliferation activity, elicited cell cycle progression, and diminished apoptosis of HB cells. On the contrary, weakened cell proliferation activity, retarded cell cycle progression with G1 phase arrest, and enhanced cell apoptosis in HB cells were observed upon transfection of the HAND2-AS1 vector (all $P < 0.01$, Fig. 3C–I; Table S5). The above results imply that HAND2-AS1 overexpression impedes cell proliferation activity and cycle progression while inducing cell apoptosis of HB cells, while knockdown of HAND2-AS1 harbors the opposite effect.

3.4. HAND2-AS1 binds to CDK1

The correlation of HAND2-AS1 to CDK1 was further analyzed using GEO microarray data GSE131329 ($P < 0.001$, Fig. 4A) and our

Table 3
Prediction of the interaction between 6 differentially expressed ncRNAs and CDK1.

Gene	UniProt Accession	Protein Status	Transcript Symbol	Ensembl Transcript ID	Transcript Status	Prediction Score
CDK1	P06493	Predictions only	LINC01124-201	ENST00000409786		21.76
CDK1	P06493	Predictions only	FAM99A-202	ENST00000538190		20.02
CDK1	P06493	Predictions only	HAND2-AS1-237	ENST00000616485	TSL 2	19.12
CDK1	P06493	Predictions only	CES1P1-204	ENST00000574030	TSL 1 (best)	16.43
CDK1	P06493	Predictions only	MEG3-205	ENST00000412736	TSL 2	16.33
CDK1	P06493	Predictions only	FAM99A-201	ENST00000382167	TSL 1 (best)	16.02
CDK1	P06493	Predictions only	MEG3-206	ENST00000423456	TSL 2	15.64
CDK1	P06493	Predictions only	HIST1H2APS4-201	ENST00000362070		15.62
CDK1	P06493	Predictions only	MEG3-211	ENST00000452514	TSL 3	15.03

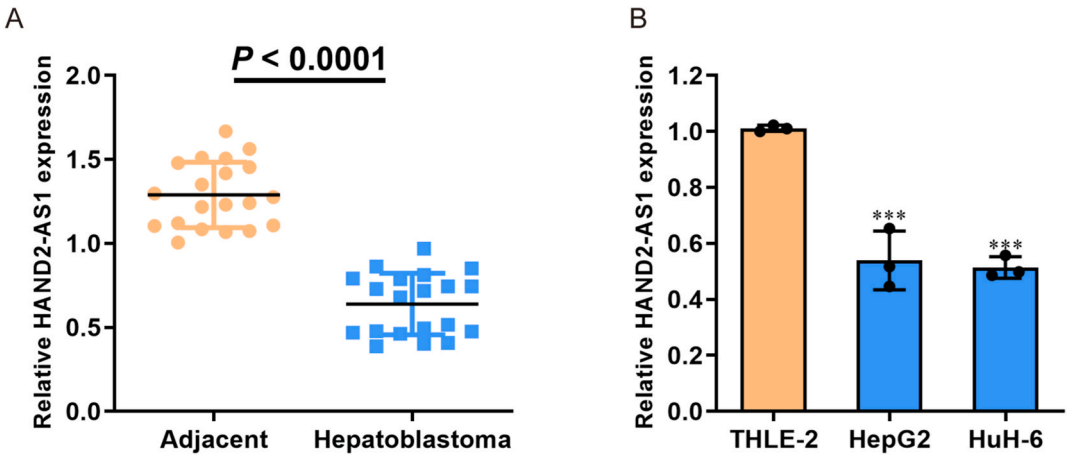

Fig. 2. HAND2-AS1 expresses at a low level in HB. A-B. qRT-PCR was utilized for the detection of HAND2-AS1 expression in HB tissues and its corresponding adjacent normal tissues; N = 20 (20 biological replicates × 3 technical replicates) (A), as well as non-malignant hepatocyte cell line THLE-2 and HB cell lines; N = 3 (3 biological replicates × 3 technical replicates) (B). ***$P < 0.001$ compared to THLE-2 group.

collected HB tissues ($P < 0.001$, Fig. 4B); HAND2-AS1 mRNA expression was negatively linked to CDK1 mRNA expression. Next, qRT-PCR and IHC were carried out to determine CDK1 mRNA and protein expression within HB tissue samples, respectively. Fig. 4C presented that CDK1 mRNA expression was upregulated in HB tissue samples when compared with paired adjacent normal tissue samples ($P < 0.001$; Table S6); Fig. 4D–E showed that CDK1 staining was markedly deepened in HB tissue samples than in adjacent non-cancerous tissue samples ($P < 0.01$; Table S6). The mRNA expression changes of CDK1 were explored by knocking down and overexpressing HAND2-AS1, respectively. An elevated CDK1 expression was observed in HB cells treated with sh-HAND2-AS1-1, while a reduced CDK1 expression was found in HB cells treated with the HAND2-AS1 vector ($P < 0.001$, Fig. 4F; Table S7). As displayed in Fig. 4G, RNA pull-down assay showed that HAND2-AS1, but not antisense HAND2-AS1, distinctively retrieved CDK1 from HuH-6 cells total protein extracts *in vitro*, indicating HAND2-AS1 could directly bind to CDK1. Then, IF combined with FISH experiments further validated the co-localization of HAND2-AS1 and CDK1 in HuH-6 cells (Fig. 4H). To identify whether HAND2-AS1 stimulates the transcription of CDK1 in the nucleus, we constructed CDK1-luc promoter plasmids. The promoter luciferase assay showed an obvious decrease in the transcriptional activity of the CDK1 promoter following HAND2-AS1 overexpression ($P = 0.01$, Fig. 4I; Table S8). Next, to confirm whether HAND2-AS1 regulates the stability of CDK1 mRNA, actinomycin D was used to achieve the inhibition of mRNA transcription. The mRNA stability of CDK1 was significantly decreased by the overexpression of HAND2-AS1 ($P < 0.001$, Fig. 4J; Table S8). Since lncRNAs may participate in the post-translational modification of target proteins, we subsequently treated cells with CHX to examine whether HAND2-AS1 could affect CDK1 protein stability. The half-life period of CDK1 was significantly reduced within cells upon the treatment of the HAND2-AS1 vector, indicating a change in its protein stability ($P < 0.001$, Fig. 4K; Table S8). The results described above revealed a negative correlation between HAND2-AS1 and CDK1 in HB, and HAND2-AS1 affected the transcriptional activity, mRNA, and protein stability of CDK1 by binding to CDK1.

3.5. HAND2-AS1 impacts HB cell proliferation, apoptosis and cycle arrest through modulating CDK1 expression

After confirming the correlation and regulation between HAND2-AS1 and CDK1, whether HAND2-AS1 could affect the malignant behaviors of HB cells by regulating CDK1 expression was investigated. First, an overexpression plasmid of CDK1 was constructed, and its overexpression effect was verified by qRT-PCR ($P < 0.001$, Fig. 5A; Table S9). Fig. 5B and Table S9 suggested that CDK1 overexpression could partially reverse the suppressive role of upregulated HAND2-AS1 in HB cell proliferation activity (all $P < 0.001$). In addition, restoration of CDK1 could partially neutralize the overexpression HAND2-AS1-caused G2 phase arrest in HB cells (all $P < 0.001$, Fig. 5C; Table S9). Meanwhile, the upregulated HAND2-AS1-induced elevation in HB cell apoptosis was partially antagonized by overexpression of CDK1 (all $P < 0.001$, Fig. 5D–E; Table S9). Furthermore, overexpression of CDK1 could partially compromise the upregulated HAND2-AS1-caused reduction of CDK1, Cyclin D1, and Cyclin B1 expression levels in HB cells (all $P < 0.001$, Fig. 5F) (Table S9). Taken together, HAND2-AS1 affects HB cell proliferation, apoptosis, and cycle progression via regulating CDK1.

4. Discussion

Nowadays, precision therapy for cancers has attracted much attention from clinical and researchers worldwide and is a hot and difficult issue in tumor research. Targeted small molecule therapy is the foundation of precision medicine and the top priority of research [25,26]. The deregulated cell cycle is one of the causes of abnormal proliferation in tumor cells. CDKs are important factors in modulating the cell cycle, and these factors are abnormally expressed in many malignant tumors, thereby contributing to the occurrence and development of tumors. Therefore, targeting CDKs can help cells return to normal cycle processes, thereby exerting functions in suppressing tumor growth and treating tumors. CDKs family proteins have become an essential target for current

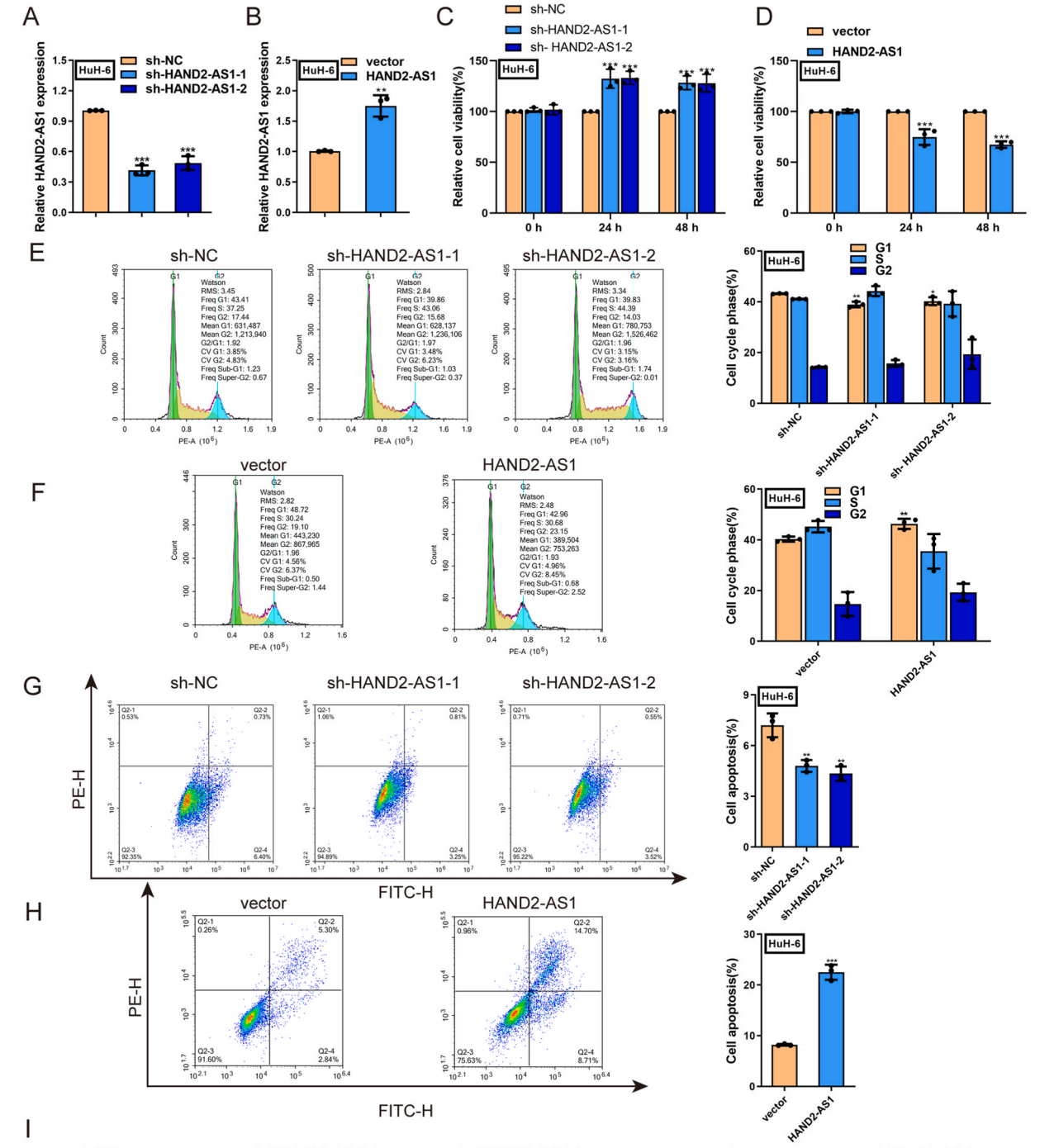

(caption on next page)

Fig. 3. Effects of HAND2-AS1 on HB cell proliferation, cycle arrest, and apoptosis. A-B. qRT-PCR was performed to validate the transfection efficiency of sh-HAND2-AS1 (A) and overexpression plasmid HAND2-AS1-vector (B). C-D. The changes in the cell proliferation activity in each treatment group were measured by MTT assay. E-F. The changes in the cell cycle arrest in each treatment group were tested by flow cytometry. G-H. The changes in the cell apoptosis in each treatment group were assessed by flow cytometry. I. DNA fragmentation in cell apoptosis was evaluated via DAPI staining. All N = 3 (3 biological replicates × 3 technical replicates), $^{*}P < 0.05$, $^{**}P < 0.01$, $^{***}P < 0.001$ compared to sh-NC or vector groups.

anti-tumor research [27]. The preliminary investigation of this group suggested that CDK1 was expressed highly in HB, but its impact and specific mechanism on HB remained unknown.

LncRNA occupies a large proportion of the human transcriptome. In the past, lncRNAs have been recognized as useless 'noise' in the transcriptome, also known as "junk RNA". With the intensive study of the human transcriptome, researchers have gradually realized that many lncRNAs exhibit aberrant expression in human malignancies and exert vital effects on tumor growth, invasion, and metastasis [28]. In this study, we screened out nine ncRNA potentially bound to CDK1 by integrative bioinformatics analyses and found the largest expression correlation |r| value between HAND2-AS1 and CDK1. Interestingly, HAND2-AS1 has been reported as a functional cancer-related lncRNA. HAND2AS1 inhibits tumor development, and its expression is decreased in cancerous tissue samples compared with that in adjacent non-cancerous tissue samples in the majority of human malignancies, such as non-small cell lung cancer [29], hepatocellular carcinoma [30], ovarian carcinoma [31], osteosarcoma [32], gastric carcinoma [33], and colorectal carcinoma [34]. In our study, we discovered for the first time that HAND2-AS1 expression is significantly lower in HB, suggesting that HAND2AS1 might also serve as a tumor suppressor in HB. As expected, the overexpression of HAND2-AS1 impeded proliferation and cell cycle progression while promoting apoptosis of HB cells, indicating the tumor-suppressive effect of HAND2-AS1 on HB.

By interacting with DNA [35], RNA [36], or protein [37], lncRNAs can influence transcription, epigenetic alterations, protein/RNA stability, translation, and post-translational modifications. As for the molecular mechanism, integrative bioinformatics analyses suggested a negative correlation between HAND2-AS1 and CDK1 expression, and our experimental results further validated the relationship between HAND2-AS1 and CDK1 expression. Specifically, HAND2-AS1 exhibited an inverse correlation with CDK1 expression in HB tissue samples, and CDK1 mRNA expression showed to be downregulated after overexpression of HAND2-AS1 in HB cells, and vice versa, implying that HAND2-AS1 may negatively regulate CDK1. Subsequently, the binding effect of HAND2-AS1 to CDK1 was further verified by RNA pull-down assay. The subcellular localization of lncRNA has important links to its function [38,39]. In the cytoplasm, lncRNAs mediate signal transduction pathways, translational programs, and posttranscriptional gene expression regulation. For example, lncRNAs can sequester proteins [40] to control their activity and levels [36,41,42], affect protein post-translational modifications [43], and govern mRNA translation and stability [44,45]. In this study, FISH experiments depicted that HAND2-AS1 co-localized with CDK1 in the cytoplasm, revealing the potential role of HAND2-AS1 in modulating CDK1 translational modification. For validating the speculation, firstly, the promoter luciferase assay showed an obvious decrease in the transcriptional activity of the CDK1 promoter following HAND2-AS1 overexpression; then, actinomycin D assay revealed the mRNA stability of CDK1 was significantly decreased by the overexpression of HAND2-AS1; finally, aycloheximide assay indicated that HAND2-AS1 could affect the protein stability of CDK1. Similarly, Gong et al. reported that HAND2-AS1 interacts with transcription factor E2F4 at the promoter of C16orf74 [46]. Liu et al. elucidated that HAND2-AS1 could negatively regulate CDK6 expression in glioma [47]. All these outcomes uncovered that HAND2-AS1 affected the transcriptional activity, mRNA, and protein stability of CDK1 by binding to CDK1. In further rescue experiments, we observed that HAND2-AS1 could negatively modulate CDK1 expression by impacting CDK1 protein stability and subsequently play a tumor suppressor role in HB.

Collectively, this study, for the first time, underlines that HAND2-AS1 expression is downregulated in HB, and the HAND2-AS1/CDK1 axis could potentially be used as a diagnostic biomarker and therapeutic target in the treatment of HB.

Ethics approval and consent to participate

This study was performed under the review and approval of the Ethics Committee of Hunan Provincial People's Hospital (2021 Scientific Research Ethics Review No: 78).

Data availability

Data are available in the publications cited in the manuscript.

Funding

This study was supported by the Research program of Health Committee of Hunan Province [202106010330], Natural Science Foundation of Hunan Province of China [2021JJ40295] and The Science and Technology Innovation Project of Hunan Province [2018SK21216].

CRediT authorship contribution statement

Keke Chen: Writing – original draft, Conceptualization. **Yalan You:** Software, Resources, Conceptualization. **Wenfang Tang:** Methodology, Investigation. **Xin Tian:** Visualization, Investigation. **Chengguang Zhu:** Formal analysis, Data curation. **Zexi Yin:**

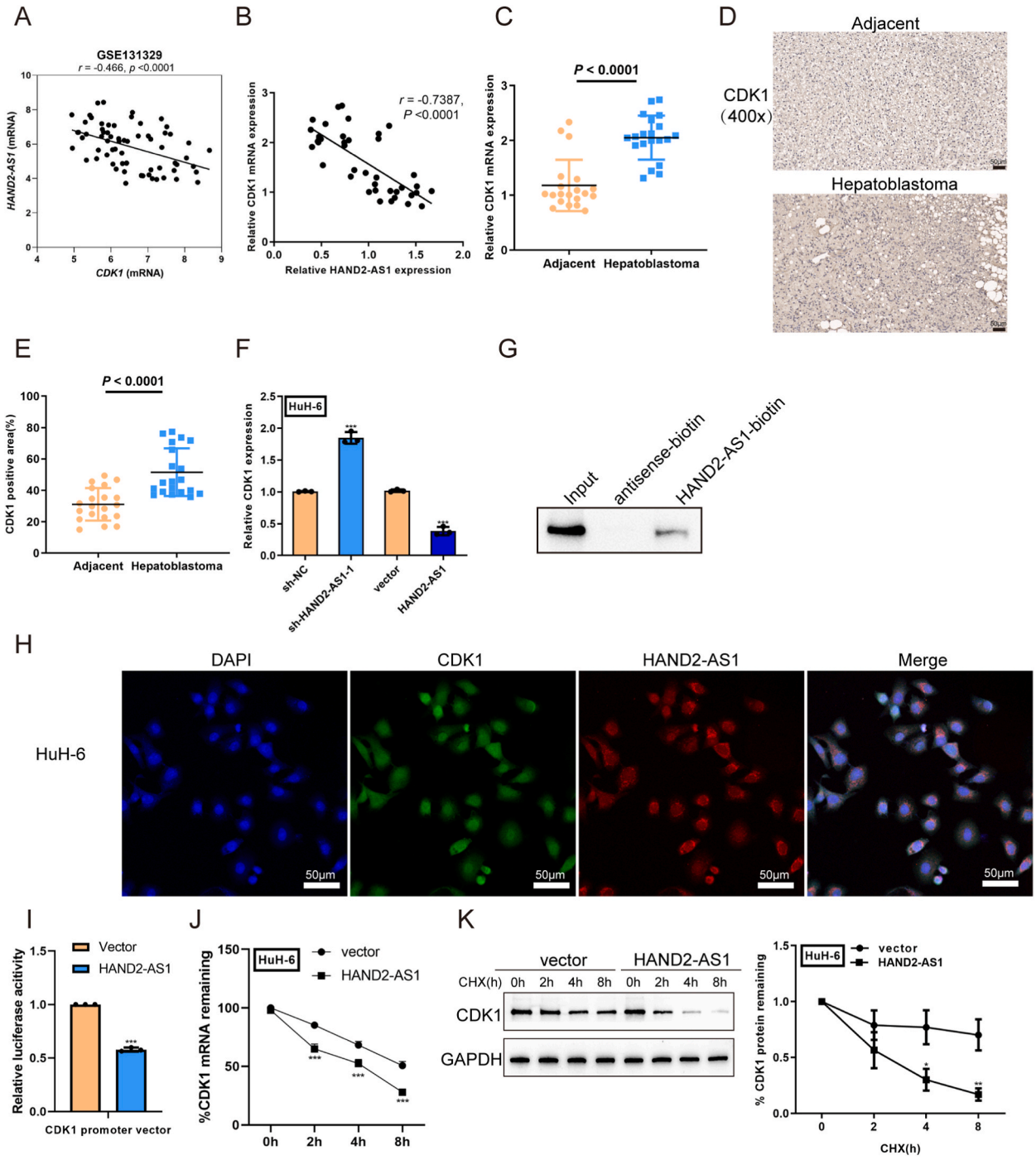

Fig. 4. HAND2-AS1 binds to CDK1 (A–B) The correlation between HAND2-AS1 mRNA and CDK1 mRNA was analyzed based on microarray datasets GSE131329 and our collected HB tissues. (C) qRT-PCR was applied to detect the CDK1 mRNA expression in HB tissues and its corresponding adjacent normal tissues. N = 20 (20 biological replicates × 3 technical replicates). (D–E) The protein expression and localization of CDK1 were detected in tissue samples by IHC staining. Scale bar = 50 μm. (F) CDK1 expression levels were determined by qRT-PCR in HB cells transduced with sh-HAND2-AS1 or overexpression plasmid HAND2-AS1-vector. (G–H) HAND2-AS1 interaction with CDK1 was validated using RNA pull-down assay (G) and FISH assay (H). Scale bar = 50 μm. (I) The luciferase activity of CDK1 promoter was evaluated by luciferase promoter assay in HAND2-AS1-overexpressing HB cells. (J) The levels of CDK1 mRNA were examined after cells were treated with actinomycin D in HAND2-AS1-overexpressed HuH-6 cells. (K) CDK1 protein stability in HB cells transduced with control vector or overexpression plasmid HAND2-AS1-vector using CHX assay. All N = 3 (3 biological replicates × 3 technical replicates), $^{*}P < 0.05$, $^{**}P < 0.01$, $^{***}P < 0.001$ compared to sh-NC or vector groups.

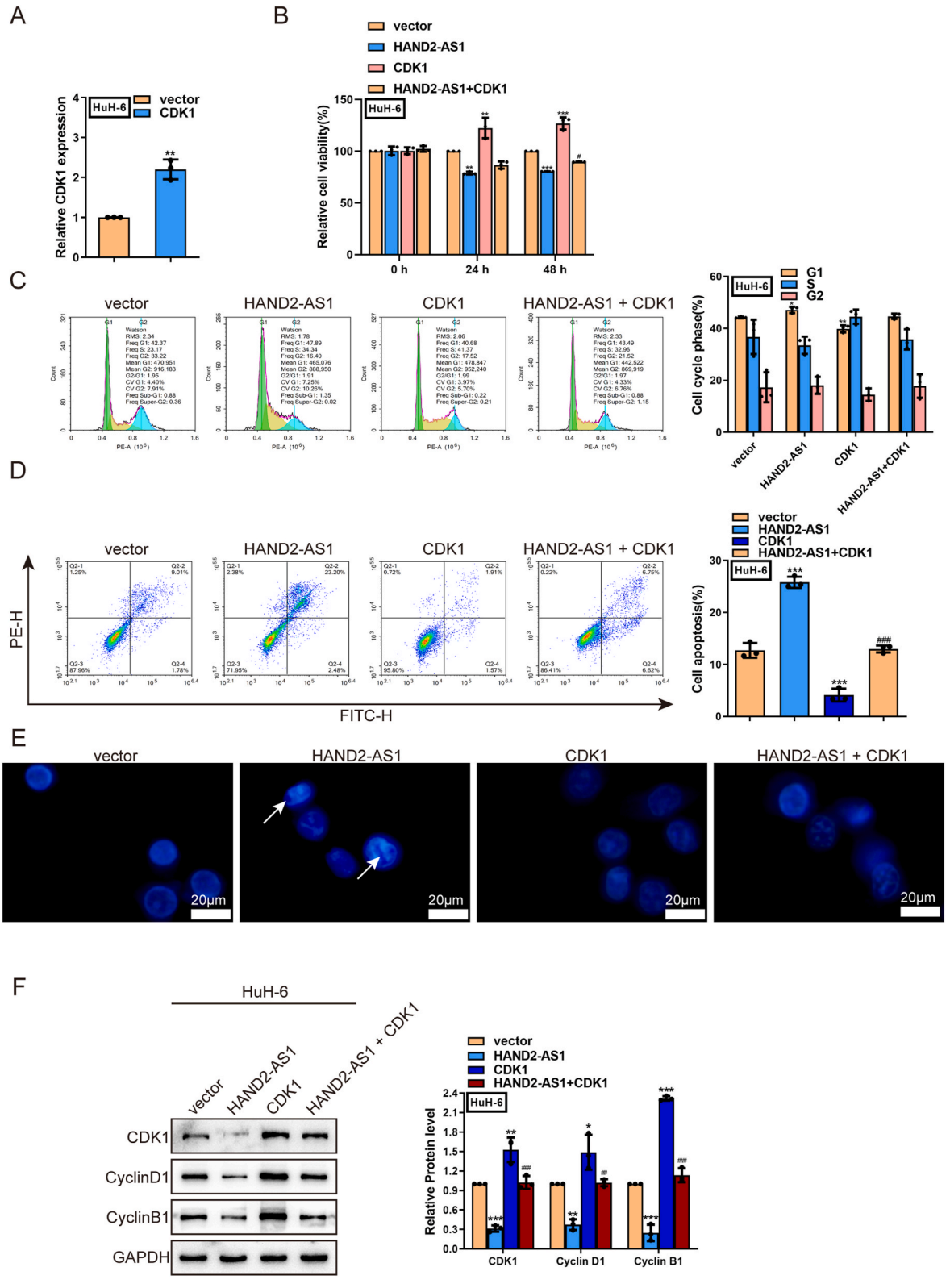

(caption on next page)

Fig. 5. HAND2-AS1 functions on HB cell proliferation, apoptosis, and cycle progression by modulating CDK1 expression. (A) The transfection effect of CDK1 overexpression plasmid was verified by qRT-PCR. (B) The changes in the cell proliferation activity in each treatment group were measured by MTT assay. (C) The changes in the cell cycle arrest in each treatment group were evaluated by flow cytometry. (D–E) The changes in the cell apoptosis in each treatment group were tested by flow cytometry and DAPI staining. (F) Expression levels of CDK1, Cyclin D1, and Cyclin B1 in HuH-6 cells of each treatment group were determined by Western blot analysis. All N = 3 (3 biological replicates × 3 technical replicates), $*P < 0.05$, $**P < 0.01$, $***P < 0.001$ compared to vector group; $\#P < 0.05$, $\#\#P < 0.01$, $\#\#\#P < 0.001$ compared to HAND2-AS1 group.

Supervision, Data curation. **Minhui Zeng:** Validation. **Xiangling He:** Writing – review & editing, Project administration, Conceptualization.

Declaration of competing interest

The authors declare that they have no known competing financial interests or personal relationships that could have appeared to influence the work reported in this paper.

Acknowledgements

None.

Appendix A. Supplementary data

Supplementary data to this article can be found online at https://doi.org/10.1016/j.heliyon.2024.e35930.

References

[1] S. Ranganathan, D. Lopez-Terrada, R. Alaggio, Hepatoblastoma and pediatric hepatocellular carcinoma: an update, Pediatr. Dev. Pathol. : the Official Journal of the Society For Pediatric Pathology and the Paediatric Pathology Society 23 (2) (2020) 79–95.
[2] J. Chou, et al., Transcription-associated cyclin-dependent kinases as targets and biomarkers for cancer therapy, Cancer Discov. 10 (3) (2020) 351–370.
[3] B. Xie, et al., Cyclin B1/CDK1-regulated mitochondrial bioenergetics in cell cycle progression and tumor resistance, Cancer Lett. 443 (2019) 56–66.
[4] J. Huang, et al., CDK1/2/5 inhibition overcomes IFNG-mediated adaptive immune resistance in pancreatic cancer, Gut 70 (5) (2021) 890–899.
[5] J.-Y. Qian, et al., KIAA1429 acts as an oncogenic factor in breast cancer by regulating CDK1 in an N6-methyladenosine-independent manner, Oncogene 38 (33) (2019) 6123–6141.
[6] R. Sun, et al., Identification of ten core hub genes as potential biomarkers and treatment target for hepatoblastoma, Front. Oncol. 11 (2021) 591507.
[7] L. Tian, et al., Integrated protein-protein interaction and weighted gene Co-expression network analysis uncover three key genes in hepatoblastoma, Front. Cell Dev. Biol. 9 (2021) 631982.
[8] A. Goga, et al., Inhibition of CDK1 as a potential therapy for tumors over-expressing MYC, Nat. Med. 13 (7) (2007) 820–827.
[9] T.R. Cech, J.A. Steitz, The noncoding RNA revolution-trashing old rules to forge new ones, Cell 157 (1) (2014) 77–94.
[10] Q. Wen, et al., lncRNA SYTL5-OT4 promotes vessel co-option by inhibiting the autophagic degradation of ASCT2, Drug Resist. Updates 69 (2023) 100975.
[11] Z. Yu, et al., Exosomal LOC85009 inhibits docetaxel resistance in lung adenocarcinoma through regulating ATG5-induced autophagy, Drug Resist. Updates 67 (2023) 100915.
[12] M.C. Bridges, A.C. Daulagala, A. Kourtidis, LNCcation: lncRNA localization and function, J. Cell Biol. 220 (2) (2021).
[13] Y. Zhang, et al., Expression and mechanism of exosome-mediated A FOXM1 related long noncoding RNA in gastric cancer, J. Nanobiotechnol. 19 (1) (2021) 133.
[14] Y. Gao, et al., Long non-coding RNA HAND2-AS1 delays cervical cancer progression via its regulation on the microRNA-21-5p/TIMP3/VEGFA axis, Cancer Gene Ther. 28 (6) (2021) 619–633.
[15] Y. Wang, et al., LncRNA HAND2-AS1 promotes liver cancer stem cell self-renewal via BMP signaling, EMBO J. 38 (17) (2019) e101110.
[16] P. Sumazin, et al., Genomic analysis of hepatoblastoma identifies distinct molecular and prognostic subgroups, Hepatology (Baltimore, Md 65 (1) (2017) 104–121.
[17] B. Lang, A. Armaos, G.G. Tartaglia, RNAct: protein-RNA interaction predictions for model organisms with supporting experimental data, Nucleic Acids Res. 47 (D1) (2019) D601–D606.
[18] Z. Tang, et al., GEPIA: a web server for cancer and normal gene expression profiling and interactive analyses, Nucleic Acids Res. 45 (W1) (2017).
[19] N. Sadeghiyeh, et al., MicroRNA-145 replacement effect on growth and migration inhibition in lung cancer cell line, Biomed. Pharmacother. 111 (2019) 460–467.
[20] M.C. Carou, et al., Apoptosis in ovarian granulosa cells of cattle: morphological features and clearance by homologous phagocytosis, Acta Histochem. 117 (1) (2015) 92–103.
[21] Y. Liang, et al., LncRNA CASC9 promotes esophageal squamous cell carcinoma metastasis through upregulating LAMC2 expression by interacting with the CREB-binding protein, Cell Death Differ. 25 (11) (2018) 1980–1995.
[22] Y. Zhou, et al., HIF1A activates the transcription of lncRNA RAET1K to modulate hypoxia-induced glycolysis in hepatocellular carcinoma cells via miR-100-5p, Cell Death Dis. 11 (3) (2020) 176.
[23] K. Pan, Y. Xie, LncRNA FOXC2-AS1 enhances FOXC2 mRNA stability to promote colorectal cancer progression via activation of Ca2+-FAK signal pathway, Cell Death Dis. 11 (6) (2020) 434.
[24] H. Xu, et al., SUMO1 modification of methyltransferase-like 3 promotes tumor progression via regulating Snail mRNA homeostasis in hepatocellular carcinoma, Theranostics 10 (13) (2020) 5671–5686.
[25] Y.T. Lee, Y.J. Tan, C.E. Oon, Molecular targeted therapy: treating cancer with specificity, Eur. J. Pharmacol. 834 (2018) 188–196.
[26] P. Gotwals, et al., Prospects for combining targeted and conventional cancer therapy with immunotherapy, Nat. Rev. Cancer 17 (5) (2017) 286–301.
[27] M. Ingham, G.K. Schwartz, Cell-cycle therapeutics come of age, J. Clin. Oncol. : Official Journal of the American Society of Clinical Oncology 35 (25) (2017) 2949–2959.
[28] A. Bhan, M. Soleimani, S.S. Mandal, Long noncoding RNA and cancer: a new paradigm, Cancer Res. 77 (15) (2017) 3965–3981.
[29] F. Miao, et al., LncRNA HAND2-AS1 inhibits non-small cell lung cancer migration, invasion and maintains cell stemness through the interactions with TGF-beta1, Biosci. Rep. 39 (1) (2019).

[30] L. Jiang, et al., lncRNA HAND2AS1 mediates the downregulation of ROCK2 in hepatocellular carcinoma and inhibits cancer cell proliferation, migration and invasion, Mol. Med. Rep. 21 (3) (2020) 1304–1309.
[31] P. Gokulnath, et al., Long non-coding RNA HAND2-AS1 acts as a tumor suppressor in high-grade serous ovarian carcinoma, Int. J. Mol. Sci. 21 (11) (2020).
[32] S. Chen, et al., Long non-coding RNA HAND2-AS1 targets glucose metabolism and inhibits cancer cell proliferation in osteosarcoma, Oncol. Lett. 18 (2) (2019) 1323–1329.
[33] Z. Xu, et al., HAND2-AS1 inhibits gastric adenocarcinoma cells proliferation and aerobic glycolysis via miRNAs sponge, Cancer Manag. Res. 12 (2020) 3053–3068.
[34] J. Zhou, et al., LncRNA HAND2-AS1 sponging miR-1275 suppresses colorectal cancer progression by upregulating KLF14, Biochem. Biophys. Res. Commun. 503 (3) (2018) 1848–1853.
[35] R. Arora, et al., RNaseH1 regulates TERRA-telomeric DNA hybrids and telomere maintenance in ALT tumour cells, Nat. Commun. 5 (2014) 5220.
[36] S. Grelet, et al., A regulated PNUTS mRNA to lncRNA splice switch mediates EMT and tumour progression, Nat. Cell Biol. 19 (9) (2017) 1105–1115.
[37] T. Yamazaki, et al., Functional domains of NEAT1 architectural lncRNA induce paraspeckle assembly through phase separation, Mol Cell 70 (6) (2018) 1038–1053 e7.
[38] L. Statello, et al., Gene regulation by long non-coding RNAs and its biological functions, Nat. Rev. Mol. Cell Biol. 22 (2) (2021) 96–118.
[39] M.C. Bridges, A.C. Daulagala, A. Kourtidis, LNCcation: lncRNA localization and function, J. Cell Biol. 220 (2) (2021).
[40] S. Lee, et al., Noncoding RNA NORAD regulates genomic stability by sequestering PUMILIO proteins, Cell 164 (1–2) (2016) 69–80.
[41] Z. Du, et al., Integrative analyses reveal a long noncoding RNA-mediated sponge regulatory network in prostate cancer, Nat. Commun. 7 (2016) 10982.
[42] J. Song, et al., A long non-coding RNA, GAS5, plays a critical role in the regulation of miR-21 during osteoarthritis, J. Orthop. Res. 32 (12) (2014) 1628–1635.
[43] A. Lin, et al., The LINK-A lncRNA activates normoxic HIF1alpha signalling in triple-negative breast cancer, Nat. Cell Biol. 18 (2) (2016) 213–224.
[44] C. Carrieri, et al., Long non-coding antisense RNA controls Uchl1 translation through an embedded SINEB2 repeat, Nature 491 (7424) (2012) 454–457.
[45] J.H. Yuan, et al., The MBNL3 splicing factor promotes hepatocellular carcinoma by increasing PXN expression through the alternative splicing of lncRNA-PXN-AS1, Nat. Cell Biol. 19 (7) (2017) 820–832.
[46] J. Gong, et al., LncRNA HAND2-AS1 represses cervical cancer progression by interaction with transcription factor E2F4 at the promoter of C16orf74, J. Cell Mol. Med. 24 (11) (2020) 6015–6027.
[47] S. Liu, Y. Li, LncRNA HAND2-AS1 attenuates glioma cell proliferation, invasion and migration by targeting CDK6, Neurol. Res. 44 (8) (2022) 677–683.